

Multi-Stage Airway Segmentation in Lung CT Based on Multi-scale Nested Residual UNet

Bingyu Yang^{1,2}, Huai Liao³, Xinyan Huang³, Qingyao Tian^{1,2}, Jinlin Wu^{1,4}, Jingdi Hu³, and Hongbin Liu^{1,4,5,*}

¹State Key Laboratory of Multimodal Artificial Intelligence Systems, Institute of Automation, Chinese Academy of Sciences, Beijing, China

²School of Artificial Intelligence, University of Chinese Academy of Sciences, Beijing, China

³Department of Pulmonary and Critical Care Medicine, The First Affiliated Hospital of Sun Yat-sen University, Guangzhou, Guangdong, China

⁴Centre of AI and Robotics (CAIR), Hong Kong Institute of Science & Innovation, Chinese Academy of Sciences, Hong Kong, China

⁵School of Engineering and Imaging Sciences, King's College London, UK

Abstract—Accurate and complete segmentation of airways in chest CT images is essential for the quantitative assessment of lung diseases and the facilitation of pulmonary interventional procedures. Although deep learning has led to significant advancements in medical image segmentation, maintaining airway continuity remains particularly challenging. This difficulty arises primarily from the small and dispersed nature of airway structures, as well as class imbalance in CT scans. To address these challenges, we designed a Multi-scale Nested Residual UNet (MNR-UNet), incorporating multi-scale inputs and Residual Multi-scale Modules (RMM) into a nested residual framework to enhance information flow, effectively capturing the intricate details of small airways and mitigating gradient vanishing. Building on this, we developed a three-stage segmentation pipeline to optimize the training of the MNR-UNet. The first two stages prioritize high accuracy and sensitivity, while the third stage focuses on repairing airway breakages to balance topological completeness and correctness. To further address class imbalance, we introduced a weighted Breakage-Aware Loss (wBAL) to heighten focus on challenging samples, penalizing breakages and thereby extending the length of the airway tree. Additionally, we proposed a hierarchical evaluation framework to offer more clinically meaningful analysis. Validation on both in-house and public datasets demonstrates that our approach achieves superior performance in detecting more accurate airway voxels and identifying additional branches, significantly improving airway topological completeness. The code will be released publicly following the publication of the paper.

Index Terms—Airway segmentation, Multi-stage training, Multi-scale Nested Residual UNet, weighted Breakage-Aware loss

I. INTRODUCTION

Chronic Respiratory Diseases (CRD), including Chronic Obstructive Pulmonary Disease (COPD), asthma, Interstitial Lung Disease (ILD), and sarcoidosis, remain leading causes of mortality worldwide [1]. With advancements in computer technology and medical imaging, Computed Tomography (CT) has become vital for diagnosing and evaluating these diseases. Accurate CT-based airway segmentation and reconstruction are essential for preoperative planning and real-time navigation,

particularly in detecting peripheral pulmonary lesions [2]. However, the complexity of pulmonary airway structures in CT images makes manual segmentation time-consuming and prone to errors.

Over the past two decades, traditional methods for airway segmentation, such as threshold segmentation [3], morphological processing [4], region growing [5], and template matching [6], have been used. Yet, due to their lack of semantic features, these methods often fail to achieve complete segmentation. Recently, deep learning has revolutionized medical image processing, with many researchers employing deep convolutional networks [7]–[13] to automatically segment airway structures in lung CT images. Compared to traditional approaches, deep learning can better mitigate airway leakage and improve overlap accuracy. However, in clinical practice, only the largest connected airway component is typically used for localization and navigation during bronchoscopic interventions, making segmentation continuity critical. Despite advancements, achieving complete and continuous airway segmentation remains challenging.

Complexity of airway structures. The lung airways form a tree-like topology with branches of varying scales, from the trachea to small airways [14]. These varying sizes challenge segmentation algorithms, as the small size of distal airways and imaging noise reduce contrast between the airway lumen and wall, leading to feature vanishing during CNN propagation. This results in segmentation discontinuities and false negatives, as shown in Fig. 1. Deep learning networks must improve multi-scale feature extraction and contextual information capture to maintain airway integrity and continuity.

Class imbalance. Pulmonary CT images exhibit significant class imbalance (airway voxels vs. background voxels) and intra-class imbalance (large airways vs. small airways). Zheng et al. [11] showed that such imbalances lead to gradient vanishing in small airways during network backpropagation, causing segmentation discontinuities. Although they introduced a new supervision method and distance-based loss function, discontinuities in small peripheral airways persist, as shown in Fig. 1.

*Corresponding author: Hongbin Liu (liuhongbin@ia.ac.cn)

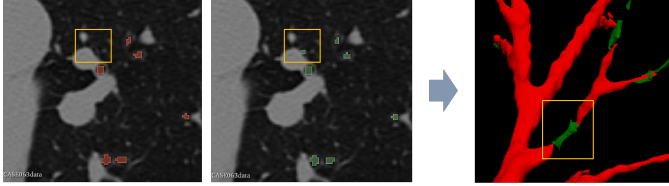


Fig. 1. Example of airway discontinuity. The red mask represents the airway prediction based on the method proposed by Zheng et al. [11], the green mask is the ground truth. Blurry airway features lead to the discontinuities (yellow box).

This highlights the need for loss functions that specifically address airway breakages.

Representativeness of evaluation metrics. Current researches often use metrics such as tree length detected rate (TD), branch detected rate (BD), Dice Similarity Coefficient (DSC), and Precision (Pre) to evaluate models [12], [13]. However, these metrics, influenced by large airways, may not accurately reflect performance in small airway segmentation.

To address these challenges, a three-stage segmentation method is proposed to improve airway topological completeness while maintaining segmentation accuracy. First, to mitigate the issue of small airway features vanishing during CNN forward propagation, the Multi-scale Nested Residual U-Net (MNR-UNet) is designed to learn airway features at various scales, enhancing the network's perception of small airways. Pyramid pooling is applied to the source input image, integrating multi-scale inputs with feature information from each level of the U-Net through residual connections. This approach improves gradient propagation within the network, and prevents the vanishing gradient problem in small airways. The U-Net's encoders are replaced with Residual Multi-scale Modules (RMMs), integrating features of different scales extracted by convolutional layers of varying depths to enrich critical information. Multi-scale nested residual computation enables MNR-UNet to more effectively capture and integrate multi-scale airway information during the encoding phase, enhancing its ability to model complex airway structures. Additionally, decoders at each level are replaced with RMMs to improve image detail recovery.

Secondly, a weighted Breakage-Aware Loss (wBAL) is proposed to address issues caused by intra-class imbalance. While distance-based loss functions focus on hard-to-segment small airways, they do not effectively address airway breakages. wBAL emphasizes the overlap between the predicted airway centerline and the ground truth centerline, assigning greater weight to centerline voxels that contribute to breakages, forcing the network to focus more on airway continuity.

In the three-stage training pipeline, the training focus is distributed as follows: extracting the main airways, mining small airways, and repairing discontinuities. Lung crop sampling is designed as network input, providing a simple yet effective hard attention for MNR-UNet training at each stage, which also helps mitigate the impact of inter-class imbalance.

Extensive experiments are conducted on a public challenge

dataset (499 cases) and an in-house dataset (55 cases), evaluating airway segmentation performance using metrics such as tree length detected rate (TD), branch detected rate (BD), Dice Similarity Coefficient (DSC), and Precision (Pre). A hierarchical evaluation concept is proposed for more clinically meaningful analysis, calculating segmentation completeness for large and small airways separately based on anatomical grading. Results demonstrate significant advantages in airway topological completeness and small airway extraction compared to other state-of-the-art methods.

II. RELATED WORK

A. Airway Segmentation

Airway segmentation is essential for diagnosing and planning surgery for pulmonary diseases. Traditional methods [3]–[6], [15] have been applied, but the EXACT'09 challenge [16] showed these approaches are inadequate for small airway extraction.

Recent advances in deep learning have enhanced automatic airway segmentation. Charbonnier et al. [7] used 2D CNNs to address airway leakage, but with limited success. The U-Net architecture has advanced the field, with Juarez et al. [8] proposing a 3D U-Net that improved feature representation but struggled with small airway detection. New modules have been introduced to improve feature extraction. Qin et al. [10] added feature recalibration and attention distillation modules, and Selvan et al. [17] treated the problem as graph refinement. However, the varying sizes of airway branches remain a challenge. Airway connectivity has also gained attention. Qin et al. [9] proposed AirwayNet to enhance voxel connectivity, and centerline tracking algorithms [18] have been developed. Zheng et al. [11] addressed class imbalance affecting connectivity with General Union Loss (GUL), though distance-based losses still struggle with airway discontinuity. Nan et al. [12] introduced JCAM loss to improve continuity.

B. Multi-scale Fusion

Multi-scale or pyramid methods are widely used in image segmentation for richer feature representation. First introduced by Burt et al. [19] in the Laplacian pyramid, this approach transforms images into a series of progressively lower-resolution images, helping the model capture diverse features at different scales.

In U-Net, multi-scale information is often integrated during the encoder or decoder stages. Techniques like image pyramid input layers or side outputs are aggregated into the U-Net framework. Abraham et al. [20] improved performance with the Focal Tversky Attention U-Net by incorporating multi-scale inputs into an attention-based U-Net with deep supervision. Similarly, Fu et al. [21] enhanced optic disc and cup segmentation in fundus images by introducing polar transformation into a U-shaped network with multi-scale inputs, enriching contextual representations. In scene parsing, Zhao et al. [22] extended this concept with a pyramid pooling module, enhancing global context and improving object size perception.

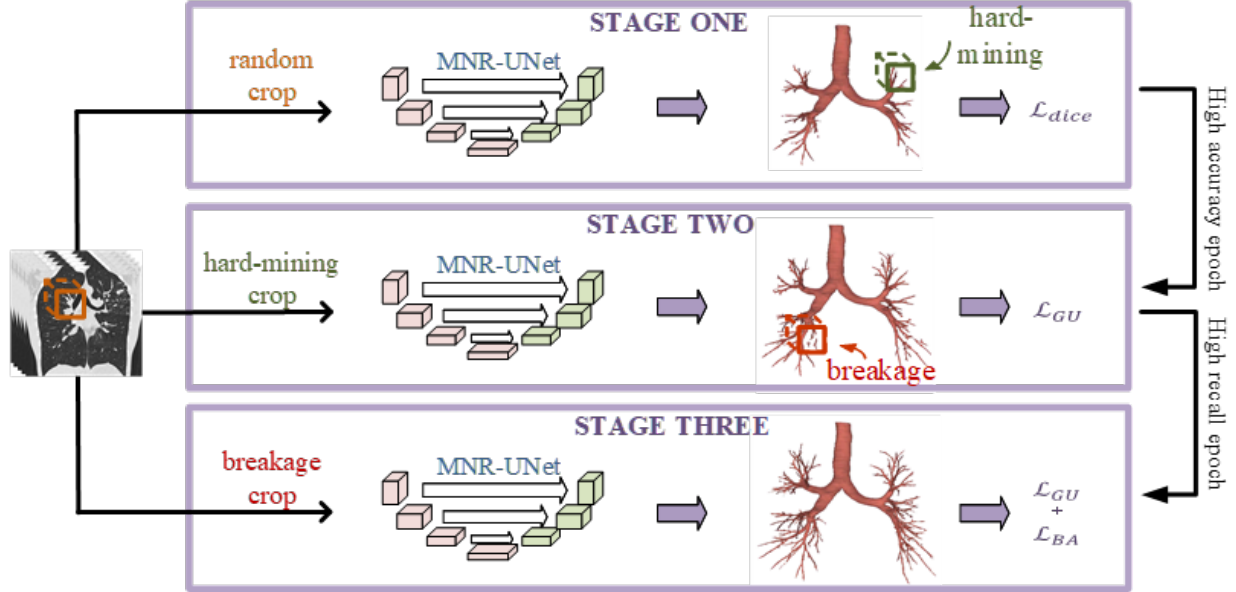


Fig. 2. The three-stage training process for airway segmentation. In “STAGE ONE”, the network is trained utilizing the Dice Loss. The epoch with the highest accuracy from the “STAGE ONE” forms the basis for the hard-mining strategy employed in the “STAGE TWO”. This stage focuses on learning to detect the challenging airways with GUL. Building upon the predictions with the highest recall from “STAGE TWO”, the “STAGE THREE” introduces wBAL to enhance the length of the airway tree. Ultimately, the optimal model is selected for segmentation testing.

III. METHOD

The three-stage training pipeline is depicted in Fig. 2. In Stage one, the network is trained to predict the main airways using random crop sampling and Dice loss [23]. The epoch with the highest accuracy serves as the foundation for the Stage two. In Stage three, General Union Loss (GUL) [11] and hard-mining crop sampling are introduced to address the challenges of small airway extraction, yielding predictions with the highest recall. Stage three is specifically designed to address discontinuities in predictions. This stage incorporates breakage crop sampling alongside a combined loss function that integrates weighted Breakage-Aware Loss (wBAL) and GUL, aiming to penalize central line voxels that compromise airway continuity, thereby extending the length of the airway tree. The optimal model from Stage three is subsequently used for testing. Details of crop sampling are provided in Section III.A, the weighted loss functions in Section III.C, and the hierarchical evaluation metrics in Section III.D.

The same network architecture shown in Fig. 3 is employed across all stages. The Multi-scale Nested Residual U-Net (MNR-UNet) is designed to enhance the learning of airway features at various scales by incorporating multi-scale inputs with feature information encoded by Residual Multi-scale Modules (RMMs). Further details on the MNR-UNet are discussed in Section III.B.

A. Crop Sampling

Given the large volume of 3D lung CT data and the constraints of GPU memory, the MNR-UNet is trained on patches extracted from lung regions, a widely adopted method [8], [12], [18]. Patch-based training serves as an effective hard

attention, mitigating the class imbalance issue in airway segmentation. However, relying exclusively on random patch sampling may not sufficiently capture crucial information.

To address this, a Hard-mining crop sampling strategy is introduced in the second stage of our training pipeline. This strategy involves randomly selecting unextracted airway skeleton points from the first stage’s predictions and generating patches containing these points, thereby increasing the network’s focus on peripheral small airways. In the third stage, Breakage crop sampling is proposed as an advanced form of Hard-mining crop sampling. This method processes the challenging airway skeleton points from the second stage using a $3 \times 3 \times 3$ all-ones convolution kernel, effectively filtering out the centerline segments associated with breakages, as illustrated in Fig. 4. Patches containing these points are then used as input to the network in the third stage.

B. Multi-scale Nested Residual UNet

The pulmonary airway structure is complex, consisting of multi-scale airway branches that pose significant challenges in feature extraction due to imaging noise and intra-class imbalance. To address these issues, we propose a novel U-Net architecture called the Multi-scale Nested Residual U-Net (MNR-UNet). This architecture achieves hierarchical residual nesting through the use of multi-scale inputs and Residual Multi-scale Modules (RMMs). The overall network structure is depicted in Fig. 3. Specifically, the 3D patches input to the network are pyramid-pooled into three resolutions, with residuals computed using a $1 \times 1 \times 1$ convolution layer and the output features from the residual multi-scale encoder at each stage. The MNR-UNet effectively captures and integrates

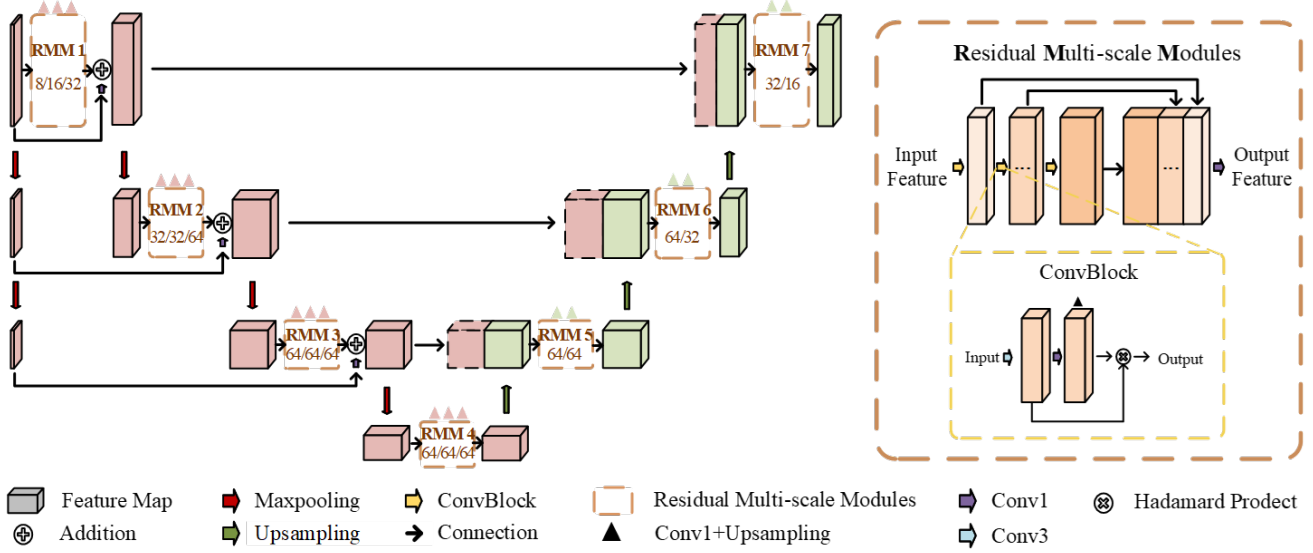


Fig. 3. The MNR-UNet architecture in proposed method. “RMM 8/16/32” refers to the output channels of the three ConvBlocks in RMM are 8, 16 and 32. The detailed structure of RMM is shown in the orange framework.

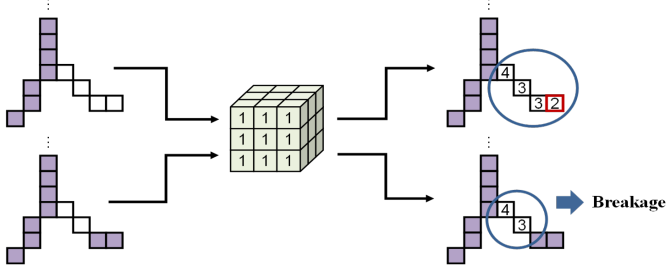


Fig. 4. Explanation of identifying airway breakages. Here shows an airway skeleton segment, with purple points representing successful predictions and white points indicating failures. A $3 \times 3 \times 3$ all-ones convolution kernel is applied to the white points to count their neighbors. If no point on a challenging airway segment has a single neighbor, it is identified as a breakage.

multi-scale airway information during the encoding phase, enhancing its ability to model complex airway structures.

The MNR-UNet comprises a total of 7 Residual Multi-scale Modules (RMMs), divided into an encoding group (RMM 1-4) and a decoding group (RMM 5-7). The RMM is an Inception-like architecture [24] that integrates multi-scale features extracted by convolutional layers of varying depths, as shown in the orange box of Fig. 3. Each RMM consists of n ConvBlocks, where each ConvBlock includes a $3 \times 3 \times 3$ convolution, a spatial attention layer, and an upsampling layer. The ConvBlock outputs features to the next block while generating an additional path through the upsampling layer, forming a group feature pyramid that is used for group supervision [11]. The RMM enriches critical information by fusing multi-scale features from several convolutional blocks through a $1 \times 1 \times 1$ convolution layer. The output of the i -th RMM to the next

module is calculated as:

$$F_{RMM_i} = \text{Conv1}(\text{Cat}(f_{i,1}, f_{i,2}, \dots, f_{i,n})), \quad (1)$$

where ‘Conv1’ is $1 \times 1 \times 1$ convolution, ‘Cat’ denotes concatenation and $f_{i,j}$ represents the feature of the j -th ConvBlock in the i -th RMM. n is the total number of blocks in this RMM (3 in the encoder and 2 in the decoder).

In encoder, the features extracted by the i -th layer are obtained by:

$$F_{en_i} = \text{Conv1}(\text{Maxpool}_i(F_{in})) \oplus F_{RMM_i}, \quad (2)$$

where ‘Maxpool $_i$ ’ represents the maxpooling at the i -th depth level and ‘ \oplus ’ denotes addition. F_{in} is the input feature and F_{RMM_i} is the output of the RMM at the i -th encoder layer (Eq. (1)).

Similarly, the features recovered by the i -th decoding layer are obtained by:

$$F_{de_i} = F_{RMM_i}. \quad (3)$$

Group supervision has been shown to effectively alleviate inter-class imbalance [11], so it is introduced for supervising the encoding and decoding groups in MNR-UNet.

C. Weighted Breakage-Aware Loss

During training, when the input patch contains both large and small airways, Dice loss tends to be dominated by the larger airways, exacerbating gradient erosion in smaller airways and making it insensitive to breakages in the results [11]. To address this, we propose a weighted Breakage-Aware Loss (wBAL), as defined in Eq. (4). This loss function penalizes voxels that are difficult to detect within the airway skeleton, placing greater emphasis on the continuity of the airway.

$$\mathcal{L}_{BA} = 1 - \frac{\sum_{i=1}^C w_i p_i g_i}{\sum_{i=1}^C w_i (p_i + g_i)}, \quad (4)$$

where C is the number of voxels on the airway centerline, p_i is the i -th skeleton voxel from the airway prediction and g_i is the ground truth. To focus on hard-to-segment small airways, w_i is written as follow:

$$w_i = w_l + w_c. \quad (5)$$

where Local-imbalance-based Weight w_l [25] adjusts the weights of airway voxels based on the size of different airway branches. To maintain branch continuity, Centerline-distance-based Weight w_c provides increased attention to points near the difficult-to-segment airway centerline, with additional weight assigned to voxels that contribute to breakage:

$$w_c = \left(1 - \frac{d_i}{d_{max}}\right)^2 + \alpha \cdot \min(1 - d_i, K), \quad (6)$$

where d_i is the shortest distance from the i -th voxel to the centerline, and d_{max} is the maximum value of d_i . α indicates whether the i -th voxel is a breakage-inducing airway voxel, as shown in Fig. 4. If it is, then $\alpha = 1$; otherwise, $\alpha = 0$. K is a hyper-parameter, and we set $K = 2$ to prevent w_c from becoming excessively large.

In the third stage of training, the hybrid loss function is expressed as shown in Eq. (7). The first stage uses Dice loss, and the second stage employs General Union loss (GUL).

$$\mathcal{L}_3 = \mathcal{L}_{GU} + \mathcal{L}_{BA}. \quad (7)$$

D. Evaluation Metrics

Based on the public benchmark for lung airway segmentation [26], we selected two categories of metrics to evaluate the airway segmentation algorithm. The first focuses on topological correctness, including Dice Similarity Coefficient (DSC,%) and Precision (Pre,%). The second focuses on topological integrity, using Tree Length Detection Rate (TD,%) and Branch Detection Rate (BD,%).

To assess performance on smaller airways, we evaluated TD and BD across different airway levels. Following the anatomical labeling from [14], we divided the airway tree into two categories: Trachea+Main Bronchi+Lobar Bronchus (gray airways after anatomy matching in Fig. 5) and Segmental Airways (colored airways). The topological analysis process, illustrated in Fig. 5, includes skeletonization and

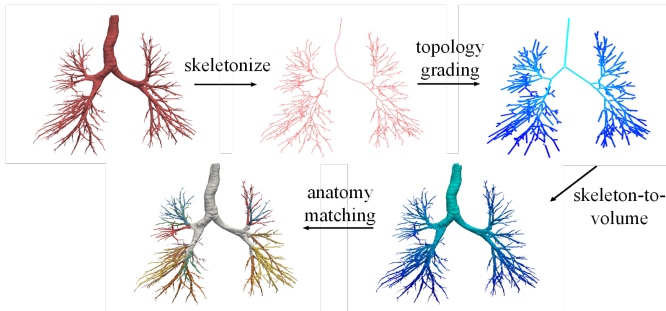


Fig. 5. A qualitative example illustrating the topological analysis process of airway tree.

Algorithm 1 Airway Skeleton Parsing and Tree Analysis

Input: Tracheal segmentation label $pred$, threshold $merge_t$
Output: Processed tracheal topology structure $airway_topo$

- 1: Perform skeletonization on $pred$ to obtain the tracheal centerline coordinate set B
- 2: Initialize branch information list $Bi = []$
- 3: **for** each point b in B **do**
- 4: **if** point b is a branch point **then**
- 5: Create a new branch $branch$
- 6: Add point b to $branch$
- 7: **Recursively** add all connected points to $branch$
- 8: Add $branch$ to Bi
- 9: **end if**
- 10: **end for**
- 11: **if** the main trachea is tortuous and complex causing segmentation errors **then**
- 12: Smooth the centerline of the main trachea and update B and Bi
- 13: **else**
- 14: Use the original B and Bi
- 15: **end if**
- 16: Optimize branches in Bi :
- 17: **for** each branch $branch$ in Bi **do**
- 18: **if** the length of branch $branch$ is $\leq merge_t$ **then**
- 19: Remove the short branch $branch$ from Bi
- 20: **end if**
- 21: **end for**
- 22: **for** each branch $branch$ in Bi **do**
- 23: **for** each other branch $other_branch$ in Bi **do**
- 24: **if** $branch$ and $other_branch$ are in a direct descendant relationship and $other_branch$ has only one parent **then**
- 25: Merge $branch$ and $other_branch$
- 26: **end if**
- 27: **end for**
- 28: **end for**
- 29: Update Bi and B to reflect the optimization results
- 30: **return** $airway_topo$ containing the processed B and Bi

parsing, skeleton topology grading, skeleton-to-volume and anatomical grading matching. For skeletonization and parsing, the extracted skeleton is first traversed, and the branch points within the skeleton are identified through topological analysis. At each branch point, the expansion begins from that point, progressively exploring along the skeleton path until either the terminal end of the airway or another branch point is reached. This process completes the initial centerline segmentation while recording the parent-child relationships between segments. Subsequently, the centerline is smoothed, with segments shorter than a predefined threshold being pruned, and single-segment parent branches are merged. This results in an accurate division of the airway branches. The detailed processing workflow is presented in Algorithm 1. The skeleton topology grading identifies branch points and

numbers them sequentially through recursive exploration of the skeleton line, while anatomical grading matching aligns the original numbering with anatomical grades based on level relationships and airway angles.

IV. EXPERIMENTS

A. Dataset

We evaluated our method on two datasets: in-house dataset used for training, assessment, and ablation studies; the ATM'22 challenge dataset [26] for fair comparative testing.

ATM'22 challenge dataset: This dataset provides 499 CT scans: 299 for training, 50 for validation, and 150 for testing [9], [11], [27], [28], sourced from EXACT'09 [16], LIDC-IDRI [29], and Shanghai Chest Hospital. Three radiologists with over five years of experience meticulously annotated the CT images. We trained our model on the train dataset, with test results evaluated by the challenge organizers.

In-house dataset: We collected and annotated 55 CT scans from The First Affiliated Hospital of Sun Yat-sen University, including samples from healthy subjects as well as patients with mild COPD and ILD. Each scan contains 256 to 612 slices, with spatial resolution ranging from 0.598 to 0.879 mm and slice thickness from 0.625 to 1.000 mm. The scans were split into training (35), validation (10), and test sets (10). Initial segmentation was done using models [11], followed by detailed annotations by three pulmonologists, finalized through majority voting.

B. Implementation Details

Data processing: Preprocessing involved truncating CT voxel intensities to [-1000, 500] and [-1024, 1024], followed by normalization to [0, 1]. Network training used CT patches sized $128 \times 128 \times 128$ as inputs. Post-processing included Dual Threshold Iteration (DTI) [30] to convert the probability map to a binary mask, morphological hole filling, and extracting the largest connected component. Thresholds in DTI were set at $T_h = 0.5$ and $T_l = 0.35$.

Model training and experimental environment: The three-stage training used the AdamW optimizer with a batch size of 8 and a learning rate of 0.0001. The network was first trained for 100 epochs with Random Crop, followed by 50 epochs using Hard-mining Crop (50%), Small Airway Crop (25%), and Random Crop (25%). The final stage comprised 50 epochs with Breakage Crop (40%), Hard-mining Crop (20%), Small Airway Crop (20%), and Random Crop (20%). The framework was implemented in PyTorch 2.0.0 and ran on an NVIDIA A800 80GB GPU.

V. RESULTS

A. Comparison Results

The ATM22 challenge organizers conducted a quantitative analysis of our method's performance on a hidden test set. Table I compares our test results with those of the top four teams in the competition, ranked by mean score. As defined in [26], the mean score is calculated as 25% TD, 25% BD, 25% DSC and 25% Precision. Our method achieved a mean

TABLE I
COMPARISON ON ATM22 TEST DATASET.

Team	TD(%)	BD(%)	DSC(%)	Pre(%)	Mean Score
timi	95.919 ±5.234	94.729 ±6.385	93.910 ±3.682	93.553 ±3.420	94.528
Proposed	96.425 ±3.156	95.479 ±4.313	93.827 ±1.897	91.781 ±4.110	94.378
YangLab	94.512 ±8.598	91.920 ±9.435	94.800 ±7.925	94.707 ±8.302	93.985
deeptree_damo	97.853 ±2.275	97.129 ±3.411	92.819 ±2.191	87.928 ±4.181	93.932
neu204	90.974 ±10.409	86.670 ±13.087	94.056 ±8.021	93.027 ±8.410	91.182

TABLE II
COMPARISON ON IN-HOUSE DATASET.* REFERS TO RESULTS OBTAINED BY AN OPEN-SOURCE MODULE (WITH TRAINED WEIGHTS). † INDICATES THE RESULTS OBTAINED BY MODULES TRAINED FROM OPEN-SOURCE CODES. THE BEST RESULT IS BOLDED, AND THE SECOND-BEST DATA IS UNDERLINED.

Method	TD(%)	BD(%)	DSC(%)	Pre(%)
3D UNet [31]*	28.419 ±16.187	25.685 ±16.047	51.401 ±16.159	91.920 ±5.427
Juarez et al. [8]*	35.323 ±25.621	32.359 ±24.260	38.095 ±26.726	80.244 ±11.289
Isensee et al. [32]†	82.453 ±11.817	72.019 ±14.990	93.132 ±4.065	92.931 ±7.323
Qin et al. [33]*	86.300 ±11.571	81.783 ±15.655	88.755 ±3.373	89.870 ±4.340
Zheng et al. [11]*	<u>89.296</u> ±2.872	<u>84.739</u> ±4.389	88.904 ±10.015	90.814 ±6.769
Proposed	92.784 ±3.665	90.040 ±5.7327	91.488 ±1.230	87.190 ±2.322

score of 94.378, ranking second only to the timi team. Notably, our method outperformed timi in TD (96.425%) and BD (95.479%) scores. Although our precision score (91.781%) was slightly lower, we attribute this to our method's ability to detect more peripheral branches, which may not be fully annotated in the test set. Compared to other teams, our TD and BD scores were 1.9% and 3.6% higher than the YangLab team, and 5.5% and 8.8% higher than the neu204 team. The deeptree_damo team, in their pursuit of higher airway completeness, sacrificed precision, resulting in the lowest DSC (92.819%) and Precision scores (87.928%). Overall, our method strikes an excellent balance between airway accuracy and completeness, achieving a high mean score.

The evaluation results on the in-house dataset, shown in Table II. Our method are compared with other state-of-the-art methods, achieving the highest TD (92.784%), BD (90.040%) and the second-highest DSC at 91.488%. The nnUNet by Isensee et al. [32] achieved the highest DSC (93.132%) and Precision (92.931%), but it does not specifically address airway segmentation challenges, resulting in poorer airway continuity. Qin et al. [33] combined 3D UNet with an attention distillation module, achieving TD (86.300%) and BD (81.783%) by improving peripheral small airway detection. Zheng et al. [11] introduced General Union Loss (GUL) and a new supervision to address class imbalance, achieving the

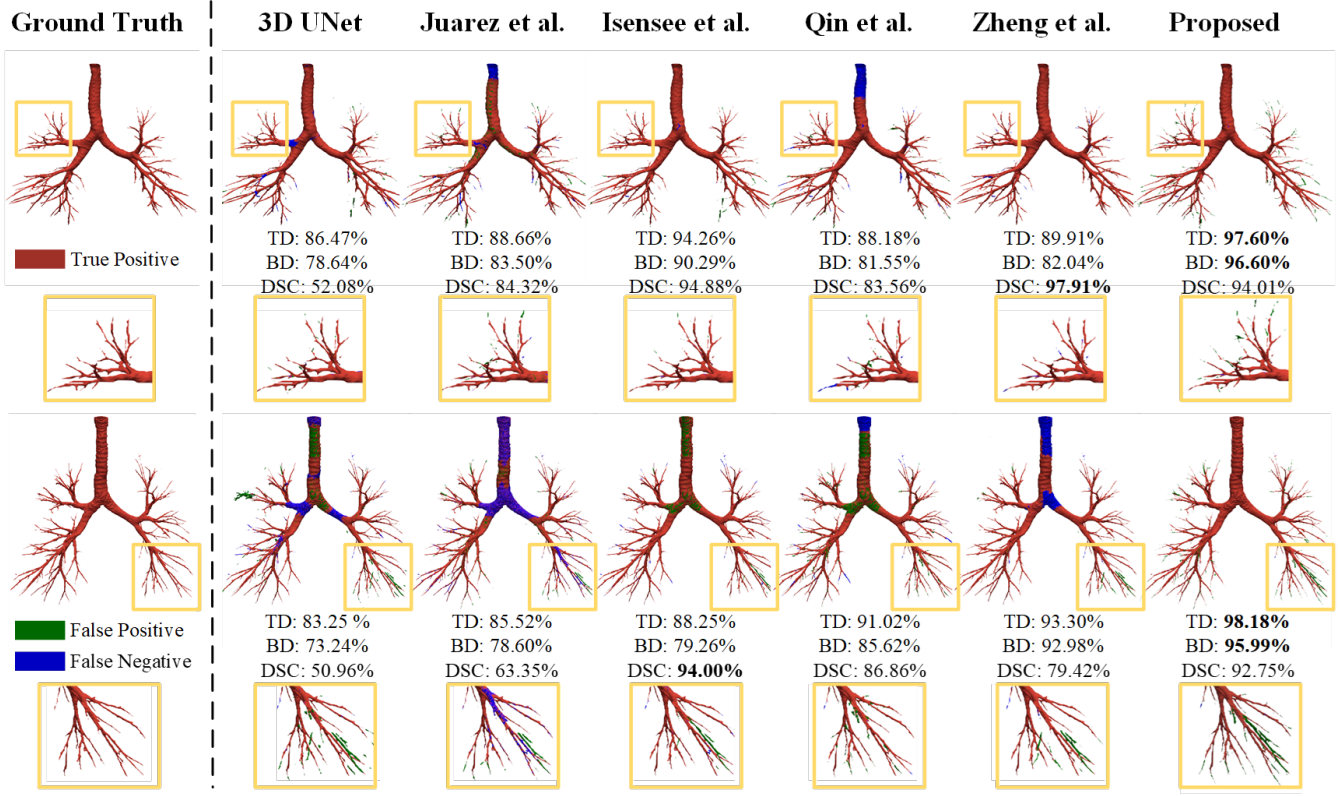


Fig. 6. Visualization of the segmentation results of the proposed approach and other CNN based methods. Red, green, and blue represent correct airways(true positive), airway leakages(false positive) and missing airways(false negative), respectively. Best viewed in color and magnified.

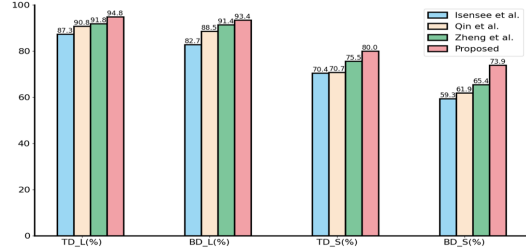


Fig. 7. The segmentation performance across different airway branch sizes.

second-highest TD (89.296%) and BD (84.739%). Methods such as 3D UNet [31] and Juarez et al. [8] exhibit more airway discontinuities. Fig. 6 illustrates test examples using various methods, highlighting our approach’s superior airway integrity and accuracy. To compare the segmentation performance across different airway branch sizes, we evaluated tree length rate TD_L, branch detection rate BD_L for large airways (Trachea, Main Bronchi, Lobar Bronchus) and TD_S, BD_S for small airways (Segmental Airways) (Fig. 5). Fig. 7 demonstrates the clear advantage of the proposed method in small airway segmentation.

B. Ablation Studies

In our in-house dataset, we conducted a detailed analysis of the proposed method’s components: (1) the importance of

TABLE III
ABLATION STUDY ON OUR DATASET. ‘WBAL’ AND ‘MNR’ ARE THE ABBREVIATIONS FOR WEIGHTED BREAKAGE-AWARE LOSS AND MULTI-SCALE NESTED RESIDUAL ARCHITECTURE. ‘MNR_EN’ AND ‘MNR_DE’ REPRESENT THE MNR IN THE ENCODER AND THE DECODER, RESPECTIVELY.

Method	TD(%)	BD(%)	DSC(%)	Pre(%)
Ours	92.784 ±3.665	90.040 ±5.733	91.488 ±1.230	87.190 ±2.322
Ours (Stage1)	71.922 ±7.993	60.286 ±8.419	93.118 ±0.867	91.593 ±0.941
Ours (Stage1+2)	88.068 ±5.734	81.550 ±8.514	92.908 ±0.943	89.309 ±1.752
Ours w/o MNR	88.358 ±5.787	82.400 ±9.767	91.868 ±0.530	87.676 ±1.105
Ours w/o MNR_en	89.066 ±5.363	83.396 ±8.110	93.038 ±1.025	89.563 ±2.013
Ours w/o MNR_de	89.529 ±5.940	83.850 ±8.718	92.918 ±0.472	89.121 ±1.091
Ours w/o wBAL	90.118 ±4.674	84.758 ±7.846	93.244 ±0.534	89.502 ±1.207

the second and third stages in the multi-stage pipeline; (2) the effectiveness of the Multi-scale Nested Residual architecture (MNR); and (3) the impact of the weighted Breakage-Aware Loss (wBAL). Table III presents the quantitative results of this ablation study.

Firstly, we compared networks trained through all three

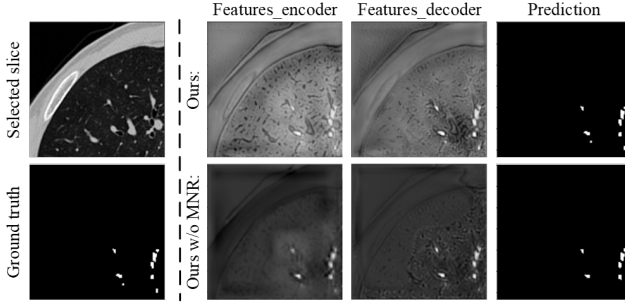


Fig. 8. The impact of the MNR architecture. The feature maps from the encoder and decoder are shown on the right.

stages with those trained through only the first stage or the first two stages. The second and third stages improved Tree Length Detection (TD) and Branch Detection (BD) by 16.146% and 4.716%, and by 21.264% and 8.490%, respectively. It shows that the second stage enhances peripheral airway detection, while the third stage further improves airway integrity by addressing discontinuities.

Secondly, we evaluated the impact of removing the MNR architecture (Fig. 8). Omitting MNR (Ours w/o MNR) slightly affected Dice Similarity Coefficient (DSC) and Precision but significantly reduced TD and BD by 4.426% and 7.640%, respectively, indicating its critical role in maintaining airway continuity and addressing intra-class imbalance. The absence of multi-scale inputs and Residual Multi-scale Modules (RMMs) in the encoding stage (Ours w/o MNR_en) notably impaired gradient propagation for small airways, affecting performance. RMMs in the decoding stage also proved essential.

Lastly, the effectiveness of wBAL was explored. The model incorporating wBAL showed improvements in TD (2.666%) and BD (5.282%), confirming that wBAL effectively encourages the network to focus on the airway breakages, thereby enhancing the segmentation accuracy.

VI. CONCLUSION

In this study, to address local discontinuities in the airway tree, we designed a Multi-scale Nested Residual U-Net (MNR-UNet) that effectively reduces information loss and improves gradient propagation. Additionally, we proposed a weighted Breakage-Aware Loss (wBAL) to tackle intra-class imbalance issues and enhance airway continuity. To balance topological completeness and accuracy, we employed a three-stage training process optimized for main airways extraction, small airways mining, and breakage repair. Experimental results on public and in-house datasets demonstrate that our method offers significant advantages in improving airway tree topological integrity and small airway extraction compared to other state-of-the-art methods.

REFERENCES

- [1] S. Momtazmanesh, S. S. Moghaddam, S.-H. Ghamari, E. M. Rad, N. Rezaei, P. Shobeiri, A. Aali, M. Abbasi-Kangevari, Z. Abbasi-Kangevari, M. Abdelmasseh *et al.*, “Global burden of chronic respiratory diseases and risk factors, 1990–2019: an update from the global burden of disease study 2019,” *EClinicalMedicine*, vol. 59, 2023.
- [2] T. Ishiwata, A. Gregor, T. Inage, and K. Yasufuku, “Bronchoscopic navigation and tissue diagnosis,” *General thoracic and cardiovascular surgery*, vol. 68, pp. 672–678, 2020.
- [3] D. Aykac, E. A. Hoffman, G. McLennan, and J. M. Reinhardt, “Segmentation and analysis of the human airway tree from three-dimensional x-ray ct images,” *IEEE transactions on medical imaging*, vol. 22, no. 8, pp. 940–950, 2003.
- [4] J. Tschirren, E. A. Hoffman, G. McLennan, and M. Sonka, “Intrathoracic airway trees: segmentation and airway morphology analysis from low-dose ct scans,” *IEEE transactions on medical imaging*, vol. 24, no. 12, pp. 1529–1539, 2005.
- [5] A. P. Kiraly, W. E. Higgins, G. McLennan, E. A. Hoffman, and J. M. Reinhardt, “Three-dimensional human airway segmentation methods for clinical virtual bronchoscopy,” *Academic radiology*, vol. 9, no. 10, pp. 1153–1168, 2002.
- [6] S. Born, D. Iwamaru, M. Pfeifle, and D. Bartz, “Three-step segmentation of the lower airways with advanced leakage-control,” in *Proc. of Second International Workshop on Pulmonary Image Analysis*. Citeseer, 2009, pp. 239–249.
- [7] J.-P. Charbonnier, E. M. Van Rikxoort, A. A. Setio, C. M. Schaefer-Prokop, B. van Ginneken, and F. Ciompi, “Improving airway segmentation in computed tomography using leak detection with convolutional networks,” *Medical image analysis*, vol. 36, pp. 52–60, 2017.
- [8] A. Garcia-Uceda Juarez, H. A. Tiddens, and M. de Bruijne, “Automatic airway segmentation in chest ct using convolutional neural networks,” in *Image Analysis for Moving Organ, Breast, and Thoracic Images: Third International Workshop, RAMBO 2018, Fourth International Workshop, BIA 2018, and First International Workshop, TIA 2018, Held in Conjunction with MICCAI 2018, Granada, Spain, September 16 and 20, 2018, Proceedings 3*. Springer, 2018, pp. 238–250.
- [9] Y. Qin, M. Chen, H. Zheng, Y. Gu, M. Shen, J. Yang, X. Huang, Y.-M. Zhu, and G.-Z. Yang, “Airwaynet: a voxel-connectivity aware approach for accurate airway segmentation using convolutional neural networks,” in *International Conference on Medical Image Computing and Computer-Assisted Intervention*. Springer, 2019, pp. 212–220.
- [10] Y. Qin, H. Zheng, Y. Gu, X. Huang, J. Yang, L. Wang, and Y.-M. Zhu, “Learning bronchiole-sensitive airway segmentation cnns by feature recalibration and attention distillation,” in *International Conference on Medical Image Computing and Computer-Assisted Intervention*. Springer, 2020, pp. 221–231.
- [11] H. Zheng, Y. Qin, Y. Gu, F. Xie, J. Yang, J. Sun, and G.-Z. Yang, “Alleviating class-wise gradient imbalance for pulmonary airway segmentation,” *IEEE transactions on medical imaging*, vol. 40, no. 9, pp. 2452–2462, 2021.
- [12] Y. Nan, J. Del Ser, Z. Tang, P. Tang, X. Xing, Y. Fang, F. Herrera, W. Pedrycz, S. Walsh, and G. Yang, “Fuzzy attention neural network to tackle discontinuity in airway segmentation,” *IEEE Transactions on Neural Networks and Learning Systems*, 2023.
- [13] P. Wang, D. Guo, D. Zheng, M. Zhang, H. Yu, X. Sun, J. Ge, Y. Gu, L. Lu, X. Ye *et al.*, “Accurate airway tree segmentation in ct scans via anatomy-aware multi-class segmentation and topology-guided iterative learning,” *IEEE Transactions on Medical Imaging*, 2024.
- [14] J. Tschirren, G. McLennan, K. Palágyi, E. A. Hoffman, and M. Sonka, “Matching and anatomical labeling of human airway tree,” *IEEE transactions on medical imaging*, vol. 24, no. 12, pp. 1540–1547, 2005.
- [15] C. Bauer, H. Bischof, and R. Beichel, “Segmentation of airways based on gradient vector flow,” in *International workshop on pulmonary image analysis, Medical image computing and computer assisted intervention*, 2009, pp. 191–201.
- [16] P. Lo, B. Van Ginneken, J. M. Reinhardt, T. Yavarna, P. A. De Jong, B. Irving, C. Fetita, M. Ortner, R. Pinho, J. Sijbers *et al.*, “Extraction of airways from ct (exact’09),” *IEEE Transactions on Medical Imaging*, vol. 31, no. 11, pp. 2093–2107, 2012.
- [17] R. Selvan, T. Kipf, M. Welling, A. G.-U. Juarez, J. H. Pedersen, J. Petersen, and M. de Bruijne, “Graph refinement based airway extraction using mean-field networks and graph neural networks,” *Medical image analysis*, vol. 64, p. 101751, 2020.
- [18] Q. Meng, H. R. Roth, T. Kitasaka, M. Oda, J. Ueno, and K. Mori, “Tracking and segmentation of the airways in chest ct using a fully convolutional network,” in *Medical Image Computing and Computer-Assisted Intervention- MICCAI 2017: 20th International Conference*,

Quebec City, QC, Canada, September 11-13, 2017, Proceedings, Part II 20. Springer, 2017, pp. 198–207.

- [19] P. J. Burt and E. H. Adelson, “The laplacian pyramid as a compact image code,” in *Readings in computer vision*. Elsevier, 1987, pp. 671–679.
- [20] N. Abraham and N. M. Khan, “A novel focal tversky loss function with improved attention u-net for lesion segmentation,” in *2019 IEEE 16th international symposium on biomedical imaging (ISBI 2019)*. IEEE, 2019, pp. 683–687.
- [21] H. Fu, J. Cheng, Y. Xu, D. W. K. Wong, J. Liu, and X. Cao, “Joint optic disc and cup segmentation based on multi-label deep network and polar transformation,” *IEEE transactions on medical imaging*, vol. 37, no. 7, pp. 1597–1605, 2018.
- [22] H. Zhao, J. Shi, X. Qi, X. Wang, and J. Jia, “Pyramid scene parsing network,” in *Proceedings of the IEEE conference on computer vision and pattern recognition*, 2017, pp. 2881–2890.
- [23] F. Milletari, N. Navab, and S.-A. Ahmadi, “V-net: Fully convolutional neural networks for volumetric medical image segmentation,” in *2016 fourth international conference on 3D vision (3DV)*. Ieee, 2016, pp. 565–571.
- [24] C. Szegedy, W. Liu, Y. Jia, P. Sermanet, S. Reed, D. Anguelov, D. Erhan, V. Vanhoucke, and A. Rabinovich, “Going deeper with convolutions,” in *Proceedings of the IEEE conference on computer vision and pattern recognition*, 2015, pp. 1–9.
- [25] H. Zheng, Y. Qin, Y. Gu, F. Xie, J. Sun, J. Yang, and G.-Z. Yang, “Refined local-imbalance-based weight for airway segmentation in ct,” in *International Conference on Medical Image Computing and Computer-Assisted Intervention*. Springer, 2021, pp. 410–419.
- [26] M. Zhang, Y. Wu, H. Zhang, Y. Qin, H. Zheng, W. Tang, C. Arnold, C. Pei, P. Yu, Y. Nan *et al.*, “Multi-site, multi-domain airway tree modeling,” *Medical Image Analysis*, vol. 90, p. 102957, 2023.
- [27] W. Yu, H. Zheng, M. Zhang, H. Zhang, J. Sun, and J. Yang, “Break: Bronchi reconstruction by geodesic transformation and skeleton embedding,” in *2022 IEEE 19th International Symposium on Biomedical Imaging (ISBI)*. IEEE, 2022, pp. 1–5.
- [28] M. Zhang, H. Zhang, G.-Z. Yang, and Y. Gu, “Cfda: Collaborative feature disentanglement and augmentation for pulmonary airway tree modeling of covid-19 cts,” in *Medical Image Computing and Computer Assisted Intervention–MICCAI 2022: 25th International Conference, Singapore, September 18–22, 2022, Proceedings, Part I*. Springer, 2022, pp. 506–516.
- [29] S. G. Armato III, G. McLennan, L. Bidaut, M. F. McNitt-Gray, C. R. Meyer, A. P. Reeves, B. Zhao, D. R. Aberle, C. I. Henschke, E. A. Hoffman *et al.*, “The lung image database consortium (lidc) and image database resource initiative (idri): a completed reference database of lung nodules on ct scans,” *Medical physics*, vol. 38, no. 2, pp. 915–931, 2011.
- [30] W. Liu, H. Yang, T. Tian, Z. Cao, X. Pan, W. Xu, Y. Jin, and F. Gao, “Full-resolution network and dual-threshold iteration for retinal vessel and coronary angiograph segmentation,” *IEEE Journal of Biomedical and Health Informatics*, vol. 26, no. 9, pp. 4623–4634, 2022.
- [31] Ö. Çiçek, A. Abdulkadir, S. S. Lienkamp, T. Brox, and O. Ronneberger, “3d u-net: learning dense volumetric segmentation from sparse annotation,” in *Medical Image Computing and Computer-Assisted Intervention–MICCAI 2016: 19th International Conference, Athens, Greece, October 17–21, 2016, Proceedings, Part II 19*. Springer, 2016, pp. 424–432.
- [32] F. Isensee, P. F. Jaeger, S. A. Kohl, J. Petersen, and K. H. Maier-Hein, “nnu-net: a self-configuring method for deep learning-based biomedical image segmentation,” *Nature methods*, vol. 18, no. 2, pp. 203–211, 2021.
- [33] Y. Qin, H. Zheng, Y. Gu, X. Huang, J. Yang, L. Wang, F. Yao, Y.-M. Zhu, and G.-Z. Yang, “Learning tubule-sensitive cnns for pulmonary airway and artery-vein segmentation in ct,” *IEEE transactions on medical imaging*, vol. 40, no. 6, pp. 1603–1617, 2021.